

Integrin $\alpha 1$ Has a Long Helix, Extending from the Transmembrane Region to the Cytoplasmic Tail in Detergent Micelles

Chaohua Lai¹, Xiaoxi Liu¹, Changlin Tian^{1,2*}, Fangming Wu^{2*}

1 Hefei National Laboratory for Physical Science at Microscale and School of Life Sciences, University of Science and Technology of China, Hefei, Anhui, China, **2** High Magnetic Field Laboratory, Chinese Academy of Sciences, Hefei, Anhui, China

Abstract

Integrin proteins are very important adhesion receptors that mediate cell-cell and cell-extracellular matrix interactions. They play essential roles in cell signaling and the regulation of cellular shape, motility, and the cell cycle. Here, the transmembrane and cytoplasmic (TMC) domains of integrin $\alpha 1$ and $\beta 1$ were over-expressed and purified in detergent micelles. The structure and backbone relaxations of $\alpha 1$ -TMC in LDAO micelles were determined and analyzed using solution NMR. A long helix, extending from the transmembrane region to the cytoplasmic tail, was observed in $\alpha 1$ -TMC. Structural comparisons of $\alpha 1$ -TMC with reported αIIb -TMC domains indicated different conformations in the transmembrane regions and cytoplasmic tails. An NMR titration experiment indicated weak interactions between $\alpha 1$ -TMC and $\beta 1$ -TMC through several $\alpha 1$ -TMC residues located at its N-terminal juxta-transmembrane region and C-terminal extended helix region.

Citation: Lai C, Liu X, Tian C, Wu F (2013) Integrin $\alpha 1$ Has a Long Helix, Extending from the Transmembrane Region to the Cytoplasmic Tail in Detergent Micelles. PLoS ONE 8(4): e62954. doi:10.1371/journal.pone.0062954

Editor: Neil A. Hotchin, University of Birmingham, United Kingdom

Received: November 29, 2012; **Accepted:** March 26, 2013; **Published:** April 30, 2013

Copyright: © 2013 Lai et al. This is an open-access article distributed under the terms of the Creative Commons Attribution License, which permits unrestricted use, distribution, and reproduction in any medium, provided the original author and source are credited.

Funding: This work was supported by the Chinese National High-Tech Research Grant (2006AA02A321) and the National Natural Science Foundation of China (30970577) to CT, and the National Natural Science Foundation of China (31100538) to FW. The funders had no role in study design, data collection and analysis, decision to publish, or preparation of the manuscript.

Competing Interests: The authors have declared that no competing interests exist.

* E-mail: cltian@ustc.edu.cn (CT); fmwu@hmfll.ac.cn (FW)

Introduction

Integrins are cell adhesion receptors that mediate cell-cell and cell-extracellular matrix interactions, regulating cell growth and function. These receptors transmit bidirectional signals across the plasma membrane and contribute to the regulation of development, immune responses, inflammation, hemostasis, and to the development of many human diseases, including infection, autoimmunity, and cancers [1,2,3,4]. They are hetero-dimeric, type I transmembrane proteins consisting of α and β subunits. Each subunit contains a relatively large extracellular domain, a single transmembrane domain (TM), and a short cytoplasmic tail (CT) [4]. In mammals, 18 α subunits and 8 β subunits can form 24 different hetero-dimers that are expressed in particular tissues and bind to particular ligands. There are two forms of integrin signaling, which are known as outside-in and inside-out signaling.

A subgroup of collagen integrin receptors, $\alpha 1/\beta 1$, $\alpha 2/\beta 1$, $\alpha 10/\beta 1$, and $\alpha 11/\beta 1$, mediate cell adhesion to extracellular matrix [5]. They have a similar collagen-binding αI domain, but have different ligand binding mechanisms and collagen subtype specificities [6,7,8]. Integrin $\alpha 1/\beta 1$ has been found to participate in the regulation of fibrosis [9], cancer-related angiogenesis [10], chronic inflammation [11], the development of myopia [12], and in the homing and differentiation of prostate cancer stem cells [2].

Structural characterizations of the extracellular domains of integrins have long been studied [13,14,15,16]. However, few studies on the transmembrane and cytoplasmic (TMC) domains of integrins have been reported. In recent years, the TM and TMC

domains of integrin αIIb and $\beta 3$ were studied, alone or in complex, in organic solvents, detergent micelles, bicelles, or lipids using NMR (nuclear magnetic resonance) methods [3,17,18,19,20,21,22]. Also, interaction interfaces between $\alpha \text{IIb}/\beta 3$ TM helices were studied using cysteine scanning and disulfide bond formation methods [23]. Multiple hydrophobic and electrostatic contacts within the membrane proximal helices of αIIb and $\beta 3$ were revealed [3]. However, very few reports about the structures of integrin $\alpha 1$ -TMC and $\beta 1$ -TMC are available.

Here, integrin $\alpha 1$ -TMC (G1135-K1179) and $\beta 1$ -TMC (V717-K798) were over-expressed using a bacterial system and purified in LDAO (lauryl-dimethylamine-n-oxide) detergent micelles. The solution structure of $\alpha 1$ -TMC in detergent micelles was determined using NMR. The structure determined showed a long helix, extending from the transmembrane region to the cytoplasmic tail of integrin $\alpha 1$ -TMC, which differed from the previously reported structure of integrin αIIb -TMC. Backbone ^{15}N relaxation data for $\alpha 1$ -TMC in LDAO micelles also confirmed the extended helix. A chemical shift perturbation study of $\alpha 1$ -TMC with the addition of integrin $\beta 1$ -TMC illustrated intensity attenuation in aqueous/membrane interfacial residues of integrin $\alpha 1$ -TMC, indicating weak interactions between integrin $\alpha 1$ -TMC and $\beta 1$ -TMC at these residues.

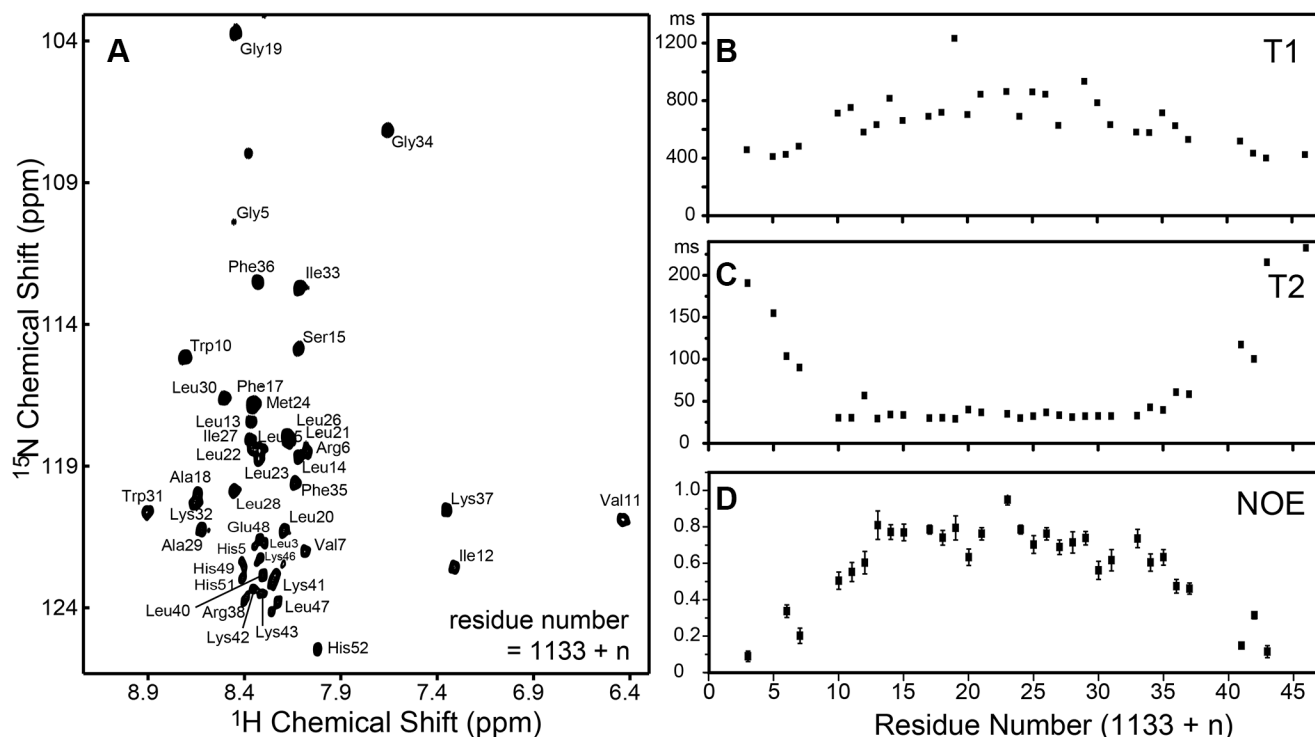


Figure 1. Resonance assignment and Backbone ^{15}N relaxation analysis of integrin $\alpha 1$ -TMC in LDAO micelles. (A) Resonance assignment of integrin $\alpha 1$ -TMC in LDAO micelles. Site-specific analysis of backbone amide ^{15}N longitudinal relaxation T1 (B), transverse relaxation T2 (C) and steady-state ^1H - ^{15}N NOE (D) of integrin $\alpha 1$ -TMC in LDAO micelles. doi:10.1371/journal.pone.0062954.g001

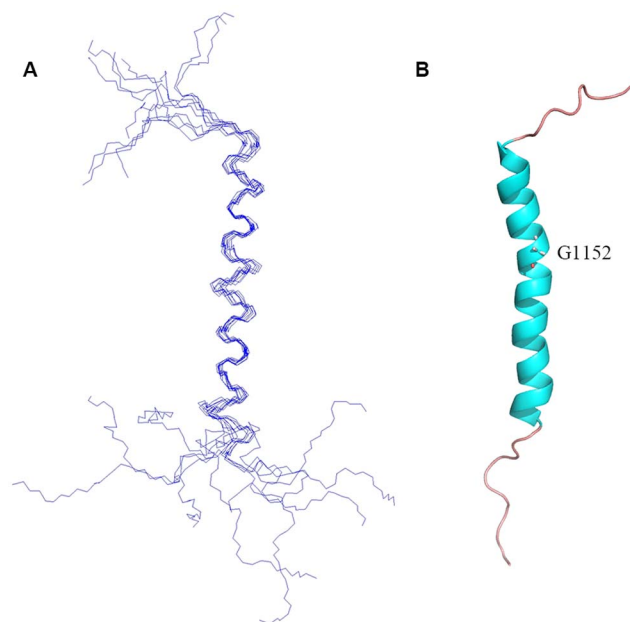


Figure 2. Solution NMR structure of human integrin $\alpha 1$ -TMC in LDAO micelles. (A) The backbone superposition of the final ten structures with the lowest energies. (B) Cartoon representation of the structure of integrin $\alpha 1$ -TMC. G1152 indicates the position of the transmembrane helix kink. doi:10.1371/journal.pone.0062954.g002

Materials and Methods

Cloning and Over-expression of Human Integrin $\alpha 1/\beta 1$ TMC

Synthetic oligonucleotides encoding integrin $\alpha 1$ -TMC (G1135-K1179) and $\beta 1$ -TMC (V717-K798) were amplified and subcloned into expression vector pET21b (Novagen) with a C-terminal 6 \times His-tag. The recombinant protein was expressed using BL21(DE3) Gold in M9 medium at 25°C for 15 h. To achieve over-expression of isotope-labeled integrin $\alpha 1$ -TMC, 1 g/L ^{15}N - NH_4Cl and 3 g/L ^{13}C -D-glucose (Cambridge Isotope Laboratory) were used as the sole nitrogen and carbon sources, respectively.

Purification of Integrin $\alpha 1/\beta 1$ TMC in Detergent Micelles

Cells were harvested by centrifugation and suspended in lysis buffer (70 mM Tris-HCl, 300 mM NaCl, pH 8.0), then lysed by sonication (Sonic and Materials), incubated with lysozyme (1.0 mg/mL), DNase (0.02 mg/mL), RNase (0.02 mg/mL), and magnesium acetate (5 mM) at 4°C for 2 h. After centrifugation, the supernatant was discarded and the pellet was washed twice in lysis buffer. The pellet was suspended in binding buffer (20 mM Tris, 100 mM NaCl, pH 8.0) in the presence of 1% SDS (sodium dodecyl sulfate) (w/v) and incubated at room temperature for 30 min, followed by centrifugation (40,000 g, 20 min, 18°C). The pellet was discarded and the supernatant was diluted using binding buffer until the concentration of SDS reached 0.2% (w/v). The protein was purified using a Ni^{2+} -NTA (Qiagen) gravity-flow column, which was washed using washing buffer (20 mM Tris, 100 mM NaCl, pH 8.0, 0.2% (w/v) SDS). Then, binding buffer with 0.2% (w/v) LDAO (Anatrace) was used to exchange detergents and achieve on-column protein refolding. Proteins

Table 1. Structural Statistics for the Final 10 Conformers of Human Integrin $\alpha 1$ -TMC.

Structural restraints	
NOE distance restraints	212
Intraresidue	58
Sequential	93
Medium-range ($2 \leq i-j \leq 4$)	61
Long-range ($ i-j \geq 5$)	0
TALOS dihedral angle constraints	60
Backbone ^1H - ^{15}N RDC	32
Total	304
Statistics for 10 structures	
RMSD from experimental restraints	
Distance	0.0530 \pm 0.0092
Dihedral	2.5069 \pm 0.2551
RMSD from idealized covalent geometry	
Bonds (\AA)	0.0021 \pm 0.0003
Angles (deg)	0.5211 \pm 0.0169
Impropers (deg)	0.5731 \pm 0.0294
Coordinate precision	
RMSD to the mean (\AA)	Backbone/Heavy atoms
Residues in secondary structure elements (9–36)	0.730/1.406
Residues of TM Helix (9–31)	0.525/1.088
Ramachandran plot statistics (%)	
Most favored regions	81.9
Additional allowed regions	11.4
Generously allowed regions	5.7
Disallowed regions	1.1

doi:10.1371/journal.pone.0062954.t001

were eluted using elution buffer (20 mM Tris, 100 mM NaCl, 0.5% LDAO, 250 mM imidazole, pH 8.0). Amicon Ultra-15 centrifugal filter units (Millipore) were used to remove imidazole and concentrate the protein. The final NMR sample contained 1.0 mM integrin $\alpha 1$ -TMC, 50 mM $\text{NaH}_2\text{PO}_4\text{-Na}_2\text{HPO}_4$ (pH 6.5), 10% (v/v) D_2O , 2 mM dithiothreitol (DTT), and 250 mM LDAO. The concentration of the protein was determined by OD₂₈₀, and the purity was analyzed using SDS-PAGE (polyacrylamide gel electrophoresis).

Solution NMR Spectroscopy of Human Integrin $\alpha 1$ -TMC

A set of multi-dimensional NMR experiments of ^{15}N - or $^{13}\text{C}/^{15}\text{N}$ -labeled integrin $\alpha 1$ -TMC were conducted at 30°C, using a 600 MHz Bruker spectrometer equipped with a TXI cryoprobe. NMR spectra, including HSQC (hetero-nuclear single quantum correlation spectroscopy), HNCQ, HNCA, HNCACB, CBCA(CO)NH, CC(CO)NH, HBHA(CO)NH, and HCC(CO)NH, were collected to obtain chemical shift assignments of backbone and side chain atoms. ^{15}N -edited NOESY-HSQC spectra (mixing time 100 ms) were collected to confirm the chemical shift assignments and to generate distance restraints for structure calculations. All NMR spectra were processed using NMRPipe [24] and analyzed using NMRView [25].

Residual Dipolar Coupling (RDC) Experiment

For backbone amide RDC measurements, a 6.5% polyacrylamide gel was prepared. Liquid gels (300 μL) will polymerize overnight at room temperature in 6-mm Teflon casting tubes. The polymerized gels were incubated for 2 h in 5 mL RDC buffer (50 mM $\text{NaH}_2\text{PO}_4\text{-Na}_2\text{HPO}_4$, pH 6.5) and then in 5 mL RDC buffer, supplemented with 0.5% LDAO and 10% D_2O . Then, the gel was incubated with 2 mL ^{15}N -labeled integrin $\alpha 1$ -TMC sample in the same detergent/buffer solution at room temperature for 2 days. The protein-soaked gel was then stretched into a 5-mm NMR tube using a device similar to that developed by the Bax group [8].

One-bond ^1H - ^{15}N RDCs [26] were measured by acquiring a pair of spectra to yield semi-TROSY (TROSY in the ^1H dimension and anti-TROSY in the ^{15}N dimension) and semi-TROSY (TROSY in the ^{15}N dimension and anti-TROSY in the ^1H dimension) resonances using ^{15}N -labeled integrin $\alpha 1$ -TMC in stretched gels. The couplings were obtained from the ^{15}N resonance frequency differences of the two semi-TROSY contour peak components.

Structure Calculations

Backbone dihedral angle restraints were obtained from the backbone chemical shifts using TALOS+ [27]. Extensive side chain NMR resonance assignments were not possible, such that the ^1H - ^1H NOEs (nuclear Overhauser effect) used to derive distance restraints for structural calculation were limited primarily to short-range backbone HN-HN distances. Backbone dihedral angle, NOE, and one-bond ^1H - ^{15}N RDC restraints were used to calculate the structure of integrin $\alpha 1$ -TMC with Xplor-NIH [28]. The final ten structures with the lowest energy were verified using PROCHECK-NMR [29]. Chemical shifts have been deposited in BioMagResBank (accession 17424). The structural coordinates have been deposited in PDB (accession 2L8S).

Backbone ^{15}N Relaxation Measurements

A ^{15}N -labeled integrin $\alpha 1$ -TMC sample was used for ^1H - ^{15}N relaxation data collection on a 500 MHz Bruker spectrometer. Backbone ^{15}N longitudinal relaxation T_1 values were determined from a series of ^1H - ^{15}N correlation spectra with 11.2, 61.6, 142, 243, 364, 525, 757, and 1150 ms relaxation evolution delays. Backbone ^{15}N transverse relaxation T_2 values were obtained from the spectra with 0, 17.6, 35.2, 52.8, 70.4, 105.6, and 140.8 ms delays. Steady-state ^1H - ^{15}N NOE values were determined from peak ratios observed between two spectra collected with or without a 3 s power presaturation in the proton channel.

NMR Titration of Integrin $\alpha 1$ -TMC with $\beta 1$ -TMC in LDAO

Non-labeled integrin $\beta 1$ -TMC was used to titrate the ^{15}N -labeled $\alpha 1$ -TMC. During the titration, the molar ratios of $\alpha 1/\beta 1$ were 1:0, 1:0.5, and 1:1. The spectra were collected on a Varian 500 MHz NMR spectrometer at 30°C.

Results and Discussion

Primary Sequence Analysis of the TMC Domains of Different Integrins

The transmembrane regions of the 18 α integrins are well-conserved, as shown in Figure S1A. Integrin $\alpha 1$ has the shortest C-terminus among all α subunits and has a specific PLKKKMEK polybasic sequence [30]. A conserved GFFKR motif in α subunits is considered to be an interaction site between integrin $\alpha 1$ and $\beta 1$, similar to the combination of hydrophobic and electrostatic

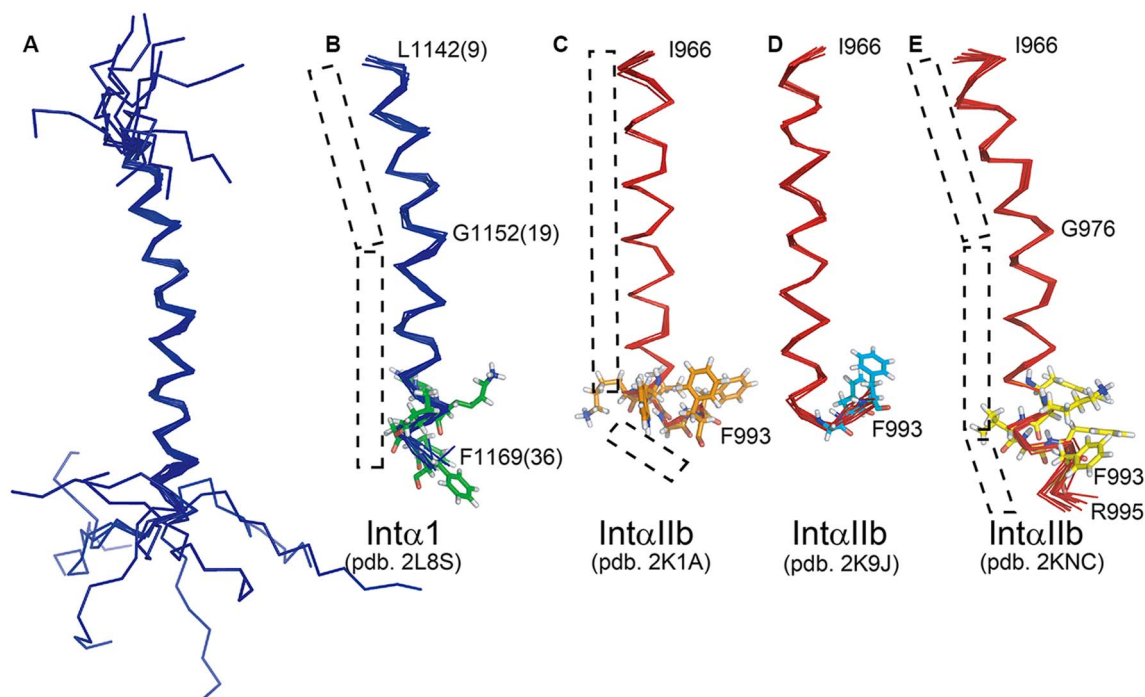


Figure 3. Structural comparison of integrin $\alpha 1$ and αIIb . Structure of $\alpha 1$ -TMC (1135–1179) and backbone structure comparisons of $\alpha 1$ -TM (1142–1169) with αIIb -TM structures indicate different bent regions in the transmembrane helix. The PDB number for each structure is listed below. (A) Structure ensemble of integrin $\alpha 1$ -TMC in LDAO micelles; (B) Structure ensemble of integrin $\alpha 1$ -TM in LDAO; (C) αIIb -TM (966–993) in bicelles [22]; (D) αIIb -TM from Int $\alpha IIb/\beta 3$ complex in bicelles [20]; (E) αIIb -TM (966–993) from $\alpha IIb/\beta 3$ complex in organic/aqueous solvents, 50% $CD_3CN/50\% H_2O$ [19].

doi:10.1371/journal.pone.0062954.g003

interactions between αIIb and $\beta 3$ [3]. This conserved GFFKR motif is known to play an important role in the regulation of integrin function, while deletion of the specific PLKKKMEK sequence has been reported to affect $\alpha 1/\beta 1$ -dependent signal transduction [30]. A tentative topology map of integrin $\alpha 1$ -TMC, including the transmembrane helix, is shown in Figure S1B, with the conserved GFFKR motif highlighted.

Solution NMR Backbone Resonance Assignment of Integrin $\alpha 1$ -TMC

A high-quality HSQC spectrum for $\alpha 1$ -TMC was obtained in LDAO micelles, which was the basis for further resonance assignments and structural determination of the protein in LDAO. With collection of a full set of triple resonance and three-dimensional solution NMR spectra, sequential resonance assignments were achieved for backbone nuclei ($^{13}C_\alpha$, $^{13}C_\beta$, ^{13}CO , amide $^{15}N/^1H$) of integrin $\alpha 1$ -TMC in LDAO micelles. The HSQC spectrum with each resonance assigned to residues of integrin $\alpha 1$ -TMC is shown in Figure 1A. In total, 43 sets of backbone carbon resonances (including ^{13}CO , $^{13}C_\alpha$ and $^{13}C_\beta$) and 38 backbone amide (1H , ^{15}N) resonances were assigned. There were still four residues (G1135, L1142, M1177, E1178) that could not be assigned, probably due to peak overlap of the narrowly dispersed HSQC spectrum of the sample in detergent micelles, or microsecond-millisecond motion of these residues.

The secondary structure of integrin $\alpha 1$ -TMC in LDAO micelles was analyzed using TALOS+ [27] from assigned chemical shift values of ^{13}CO , $^{13}C_\alpha$, $^{13}C_\beta$, amide 1H , and ^{15}N (Fig. S2). Site-specific secondary structure prediction indicated that, in total, 24 residues (L1142–K1165) were shown in an α -helix secondary

structure, corresponding to the transmembrane helix of integrin $\alpha 1$ -TMC.

Structural Calculation and Description

The solution structure of integrin $\alpha 1$ -TMC was determined using Xplor-NIH [28], based on 212 NOE, 60 dihedral angle, and 32 backbone 1H - ^{15}N RDC restraints. Ten lowest energy structures were selected out of 100 calculated structures. Structural computation statistics regarding the quality and precision of integrin $\alpha 1$ -TMC are summarized in Table 1. The backbone superimposition of the final ten conformers is presented in Figure 2A. In this structure, a kink was observed in the transmembrane helix at the position of G1152 (Fig. 2B). A stretch of helix with 28 residues was observed to extend from the transmembrane helix to the conserved GFF motif. This conformation of the integrin $\alpha 1$ -TMC domain in LDAO micelles was also consistent with the backbone ^{15}N relaxation data (Fig. 1B–D). The longitudinal relaxation T_2 values of residues W1143–F1168 were similar (about 30 ms; Fig. 1C) and their steady-state NOE values were above 0.5 (Fig. 1D), indicating that these residues (W1143–F1168) form a stable secondary structural region, flanked by two flexible terminals.

Structural Comparison of Integrin $\alpha 1$ -TMC with other Reported Integrin TMC Domains

Using solution NMR or computation modeling methods, several structures of integrin transmembrane helix (TM) and/or C-terminal tails (CT) have been determined over the past 10 years. Most of the reported integrin TM or CT structures are integrin $\alpha IIb/\beta 3$, which play important roles in primary platelet adhesion [3,19,20,21,22,31,32]. Previously, several TM or CT domain

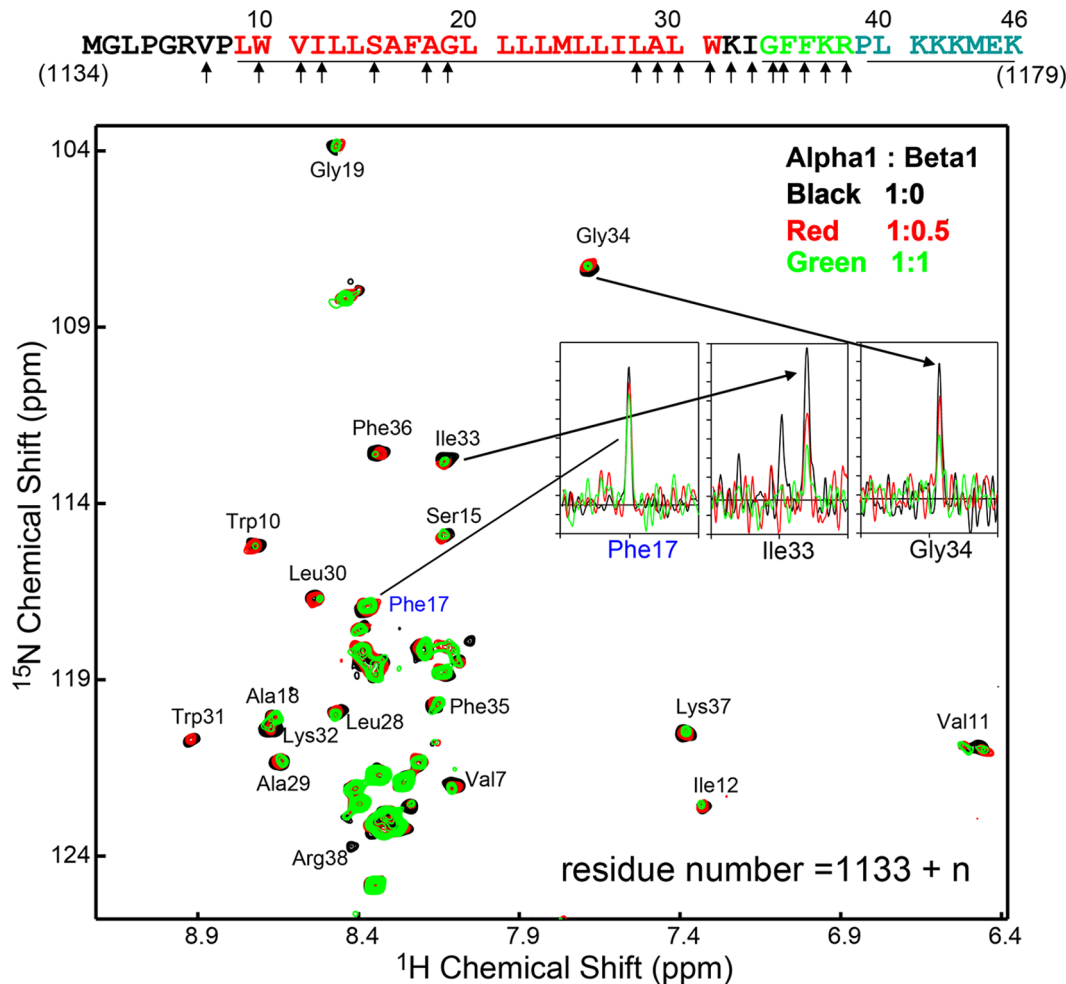


Figure 4. Chemical shift perturbation analysis of integrin $\alpha 1$ -TMC upon the addition of integrin $\beta 1$ -TMC. HSQC titration of ^{15}N -labeled integrin $\alpha 1$ -TMC with addition of unlabeled integrin $\beta 1$ -TMC. Some peaks of integrin $\alpha 1$ -TMC are missing at elevated integrin $\beta 1$ -TMC concentrations (marked with residue names). Residues with missing peaks are probably due to intermediate time-scale interactions between $\alpha 1$ -TMC/ $\beta 1$ -TMC, consistent with predicted interaction points of $\alpha 1$ and $\beta 1$. A peak intensity with little change is exemplified with F17 and missing peaks are shown for I33 and G34.

doi:10.1371/journal.pone.0062954.g004

structures of integrin $\alpha\text{IIb}/\beta 3$ have been studied in different amphipathic environments (such as detergent micelles, phospholipid bicelles) or organic solvents. Some minor structural differences were observed for the same integrin segments in the different environments.

Here, the structure of integrin $\alpha 1$ -TMC in LDAO micelles was compared with several representative structures of αIIb , such as the αIIb TM segment in bicelles (PDB: 2K1A) [22], the $\alpha\text{IIb}/\beta 3$ TM complex in bicelles (PDB: 2K9J) [20], and the $\alpha\text{IIb}/\beta 3$ TMC complex in $\text{CD}_3\text{CN}/\text{H}_2\text{O}$ (PDB: 2KNC) [19]. In Figure 3, the three αIIb structures were shown, alongside our $\alpha 1$ TMC structure. Clearly, a kink was observed in both integrin $\alpha 1$ -TMC at Gly1152 (Fig. 3B) and integrin αIIb -TMC of the $\alpha\text{IIb}/\beta 3$ TMC complex in $\text{CD}_3\text{CN}/\text{H}_2\text{O}$ (Fig. 3E, G976), while no such kink was seen in the structure of integrin αIIb -TMC in bicelles (Fig. 3C, 3D).

Notably, in the cytoplasmic region of integrin $\alpha 1$ and αIIb , the GFF (1167-GFF-1169 in $\alpha 1$ and 991-GFF-993 in αIIb) has been reported to form a helix in detergent and organic solvent (Fig. 3B, 3E) [19], or a GFF reverse turn with its two Phe residues immersed back into the hydrophobic region of bicelles (Fig. 3C, 3D) [20,22].

Moreover, the GFF helical conformation [33] and a GFF reverse turn [31,34] can be readily obtained through different computation modeling. In particular, a CS-Rosetta prediction by Yang *et al.* showed that the GFF reverse turn was the majority conformation, while the GFF helical conformation was seen in a small proportion [19]. In addition to the two different conformations of $\alpha\text{IIb}/\beta 3$ in different conditions [19,20], integrin α/β heterodimer formation efficiencies were also affected by different membrane-mimicking environments [35]. In light of these results and the complex physiological function of integrins, it is possible that integrin $\alpha 1$ -TMC could be in multiple conformations (helix or reverse turn). Transitions between different conformations could be induced by environmental changes and/or specific physiological processes (e.g., activation/inactivation or monomer/dimer formation).

On the other hand, it was previously reported that the conserved GFFKR motifs in different integrins have different correlations with their functions. For example, the αIIb F992A or F993A mutation can activate $\alpha\text{IIb}/\beta 3$ [36] while the FF/AA mutation in this motif had little effect in the activation of $\alpha\text{V}/\beta 3$ [37]. Probably, the conformations of the GFFKR motif in these

two integrins are different. Previously, it was reported that the $\alpha \text{IIb}/\beta 3$ association was sensitive to the integrity of the $\alpha \text{IIb}(\text{R995})-\beta 3(\text{D723})$ salt bridge [20,36], the KR residues in GFFKR motif having undefined structure might provide some flexibility for the salt bridge formation between integrin $\alpha 1$ and integrin $\beta 1$.

Here, an extending helical conformation of integrin $\alpha 1$ -TMC was determined using solution NMR in detergent micelles, indicating a majority helical conformation of integrin $\alpha 1$ -TMC in its monomeric form in micelles. Whether a conformation with a GFF reverse turn can be observed in the $\alpha 1/\beta 1$ complex or in lipid bilayers need to be examined in future studies.

Interactions between Integrin $\alpha 1$ -TMC and $\beta 1$ -TMC in LDAO Micelles

Interactions between the TMC domain of integrin $\alpha 1$ and $\beta 1$ are known to be important for cell adhesion, probably due to integrin clustering. The C-terminal tail of integrin $\alpha 1$ plays an essential role in both physiological and pathological angiogenesis [38]. Deletion of the entire cytoplasmic tail of integrin $\alpha 1$ or mutations in several amino acids distal to the highly conserved GFFKR motif have been reported to have a similar phenotype to parental $\alpha 1$ -null cells, resulting in malfunctions in angiogenesis and endothelial cell proliferation [38]. The highly conserved GFFKR motif in the $\alpha 1$ tail has been proposed to form a salt bridge with conserved residues in the $\beta 1$ tail. However, the detailed interaction between TMC domains of $\alpha 1$ and $\beta 1$ is not yet understood. Due to the complex enthalpy solvent effects of detergent mixing or exchange between two membrane protein samples, isothermal titration calorimetry assay is not suitable for analyzing interactions between $\alpha 1$ -TMC/ $\beta 1$ -TMC in detergent micelles. Thus, NMR titration experiment was employed to study the interaction between $\alpha 1$ -TMC and $\beta 1$ -TMC. First of all, we acquired the HSQC spectrum of $\beta 1$ -TMC to make sure it's a well folded sample (Fig. S3). Then, a series of $^1\text{H}-^{15}\text{N}$ HSQC spectra of ^{15}N -labeled integrin $\alpha 1$ -TMC with different concentrations of non-labeled $\beta 1$ -TMC were acquired and the processed spectra are shown in Figure 4. Surprisingly, no obvious chemical shift perturbation was observed anywhere in the spectrum, indicating no pronounced conformational change of integrin $\alpha 1$ -TMC upon addition of $\beta 1$ -TMC, maintaining the major helical conformation in the GFF motif. However, intensity attenuations were observed in several resonances with increasing integrin $\beta 1$ -TMC concentration (Fig. 4). These resonances with attenuated intensities were mapped to two regions: the N-terminal juxta-transmembrane region (V1140, W1143, V1144, I1145, S1148, A1151, and G1152) and the C-terminal juxta-transmembrane region (L1161, A1162, L1163, W1164, K1165, I1166, G1167, F1168, F1169, K1170, and R1171). These residues are marked with arrows at the top of Figure 4.

According to solution NMR relaxation theories, peak intensity attenuation or missing peaks are attributed to intermediate-time

scale (microsecond to millisecond) conformational exchanges [39,40,41]. Thus, intensity attenuation or the 'disappearance' of residues are hypothesized to indicate interaction and these residues are located in the direct interface between integrin $\alpha 1/\beta 1$.

This hypothesized $\alpha 1/\beta 1$ interaction interface is possibly similar to interactions in integrin $\alpha \text{IIb}/\beta 3$ and consistent with previous mutagenesis and deletion studies of integrin $\alpha 1$ [42,43,44]. In the complex structure of $\alpha \text{IIb}/\beta 3$ TMC, αIIb residues W968, G972, G976, L979, L980, and R995 are involved in the dimer interface [19,20]. Their corresponding residues in $\alpha 1$ are V1144, S1148, G1152, L1155, L1156, and R1171. Here, the HSQC peaks of four of them (V1144, S1148, G1152, R1171) were obviously attenuated in the NMR titration experiment with integrin $\beta 1$ -TMC, while perturbations of the other two residues (L1155, L1156) were not apparent because they were crowded by L1158 and I1160. Also, the $\alpha \text{IIb}/\beta 3$ residues involved in the dimer interface are largely conserved in $\alpha 1/\beta 1$. Those observations implied that the dimer interface of $\alpha 1/\beta 1$ TMC is similar to that of $\alpha \text{IIb}/\beta 3$ TMC. Further structural studies of $\alpha 1/\beta 1$ TMC complex will illustrate detail interaction surfaces. Residue mutations and deletions in the two regions have been reported to interfere with associations between α and β subunits and between integrin and cytoplasmic binding partners, thus interfering with downstream signal transduction, leading to inhibition of cell spreading and stress fiber formation [42,43,44]. Thus, titration results of integrin $\alpha 1$ with the addition of integrin $\beta 1$ -TMC provide preliminary insights about the interaction interfaces between the two proteins, and provide a basis for further detailed studies of signal transduction in fibrosis, angiogenesis, or cancer cells.

Supporting Information

Figure S1 Sequence alignment of 18 integrin α -TMCs (A) and topology of integrin $\alpha 1$ -TMC (B).
(TIF)

Figure S2 The predicted secondary structure results of each residue calculated using TALOS+.
(TIF)

Figure S3 The HSQC spectrum of $\beta 1$ -TMC.
(TIF)

Acknowledgments

The authors are grateful to Mr. Jiahai Zhang (School of Life Sciences, University of Science and Technology of China, USTC) for great maintenance of solution NMR spectrometers.

Author Contributions

Conceived and designed the experiments: CL XL CT. Performed the experiments: CL XL CT. Analyzed the data: CL CT FW. Contributed reagents/materials/analysis tools: CL CT FW. Wrote the paper: CL CT FW.

References

- Shattil SJ, Kim C, Ginsberg MH (2010) The final steps of integrin activation: the end game. *Nat Rev Mol Cell Biol* 11: 288–300.
- Rentala S, Yalavarthy PD, Mangamoori LN (2010) Alpha1 and beta1 integrins enhance the homing and differentiation of cultured prostate cancer stem cells. *Asian J Androl* 12: 548–555.
- Vinogradova O, Velyvis A, Velyviene A, Hu B, Haas T, et al. (2002) A structural mechanism of integrin alpha(IIb)beta(3) "inside-out" activation as regulated by its cytoplasmic face. *Cell* 110: 587–597.
- Hynes RO (2002) Integrins: bidirectional, allosteric signaling machines. *Cell* 110: 673–687.
- Anthos NJ, Campbell ID (2011) The tail of integrin activation. *Trends Biochem Sci* 36: 191–198.
- Tulla M, Pentikainen OT, Viitasalo T, Kapyla J, Impola U, et al. (2001) Selective binding of collagen subtypes by integrin alpha 1I, alpha 2I, and alpha 10I domains. *J Biol Chem* 276: 48206–48212.
- Zhang WM, Kapyla J, Puranen JS, Knight CG, Tiger CF, et al. (2003) alpha 1 beta 1 integrin recognizes the GFOGER sequence in interstitial collagens. *J Biol Chem* 278: 7270–7277.
- Chou JJ, Gaemers S, Howder B, Louis JM, Bax A (2001) A simple apparatus for generating stretched polyacrylamide gels, yielding uniform alignment of proteins and detergent micelles. *J Biomol NMR* 21: 377–382.
- Gardner HA (1999) Integrin signaling in fibrosis and scleroderma. *Curr Rheumatol Rep* 1: 28–33.

10. Pozzi A, Moberg PE, Miles LA, Wagner S, Soloway P, et al. (2000) Elevated matrix metalloproteinase and angiotensin levels in integrin alpha 1 knockout mice cause reduced tumor vascularization. *Proc Natl Acad Sci U S A* 97: 2202–2207.
11. Ekholm E, Hankenson KD, Uusitalo H, Hiltunen A, Gardner H, et al. (2002) Diminished callus size and cartilage synthesis in alpha 1 beta 1 integrin-deficient mice during bone fracture healing. *Am J Pathol* 160: 1779–1785.
12. McBrien NA, Metlapally R, Jobling AI, Gentle A (2006) Expression of collagen-binding integrin receptors in the mammalian sclera and their regulation during the development of myopia. *Invest Ophthalmol Vis Sci* 47: 4674–4682.
13. Xiong JP, Stehle T, Diefenbach B, Zhang R, Dunker R, et al. (2001) Crystal structure of the extracellular segment of integrin alpha Vbeta3. *Science* 294: 339–345.
14. Xiong JP, Stehle T, Zhang R, Joachimiak A, Frech M, et al. (2002) Crystal structure of the extracellular segment of integrin alpha Vbeta3 in complex with an Arg-Gly-Asp ligand. *Science* 296: 151–155.
15. Karpusas M, Ferrant J, Weinreb PH, Carmillo A, Taylor FR, et al. (2003) Crystal structure of the talin/integrin complex at a lipid bilayer in complex with an antibody Fab fragment. *J Mol Biol* 327: 1031–1041.
16. Xiong JP, Stehle T, Goodman SL, Arnaout MA (2004) A novel adaptation of the integrin PSI domain revealed from its crystal structure. *J Biol Chem* 279: 40252–40254.
17. Metcalf DG, Moore DT, Wu Y, Kielec JM, Molnar K, et al. (2010) NMR analysis of the alphaIIb beta3 cytoplasmic interaction suggests a mechanism for integrin regulation. *Proc Natl Acad Sci U S A* 107: 22481–22486.
18. Kalli AC, Wegener KL, Goult BT, Anthis NJ, Campbell ID, et al. (2010) The structure of the talin/integrin complex at a lipid bilayer: an NMR and MD simulation study. *Structure* 18: 1280–1288.
19. Yang J, Ma YQ, Page RC, Misra S, Plow EF, et al. (2009) Structure of an integrin alphaIIb beta3 transmembrane-cytoplasmic heterocomplex provides insight into integrin activation. *Proc Natl Acad Sci U S A* 106: 17729–17734.
20. Lau TL, Kim C, Ginsberg MH, Ulmer TS (2009) The structure of the integrin alphaIIb beta3 transmembrane complex explains integrin transmembrane signalling. *EMBO J* 28: 1351–1361.
21. Lau TL, Partridge AW, Ginsberg MH, Ulmer TS (2008) Structure of the integrin beta3 transmembrane segment in phospholipid bicelles and detergent micelles. *Biochemistry* 47: 4008–4016.
22. Lau TL, Dua V, Ulmer TS (2008) Structure of the integrin alphaIIb transmembrane segment. *J Biol Chem* 283: 16162–16168.
23. Luo BH, Springer TA, Takagi J (2004) A specific interface between integrin transmembrane helices and affinity for ligand. *PLoS Biol* 2: e153.
24. Delaglio F, Grzesiek S, Vuister GW, Zhu G, Pfeifer J, et al. (1995) NMRPipe: a multidimensional spectral processing system based on UNIX pipes. *J Biomol NMR* 6: 277–293.
25. Johnson BA (2004) Using NMRView to visualize and analyze the NMR spectra of macromolecules. *Methods Mol Biol* 278: 313–352.
26. Weigelt J (1998) Single Scan, Sensitivity- and Gradient-Enhanced TROSY for Multidimensional NMR Experiments. *J Am Chem Soc* 120: 10778–10779.
27. Shen Y, Delaglio F, Cornilescu G, Bax A (2009) TALOS+: a hybrid method for predicting protein backbone torsion angles from NMR chemical shifts. *J Biomol NMR* 44: 213–223.
28. Schwieters CD, Kuszewski JJ, Tjandra N, Marius Clore G (2003) The Xplor-NIH NMR molecular structure determination package. *J Magn Reson* 160: 65–73.
29. Laskowski RA, Rullmann JA, MacArthur MW, Kaptein R, Thornton JM (1996) AQUA and PROCHECK-NMR: programs for checking the quality of protein structures solved by NMR. *J Biomol NMR* 8: 477–486.
30. Smerling C, Tang K, Hofmann W, Danker K (2007) Role of the alpha(1) integrin cytoplasmic tail in the formation of focal complexes, actin organization, and in the control of cell migration. *Exp Cell Res* 313: 3153–3165.
31. Zhu J, Luo BH, Barth P, Schonbrun J, Baker D, et al. (2009) The structure of a receptor with two associating transmembrane domains on the cell surface: integrin alphaIIb beta3. *Mol Cell* 34: 234–249.
32. Weljie AM, Hwang PM, Vogel HJ (2002) Solution structures of the cytoplasmic tail complex from platelet integrin alpha IIb- and beta 3-subunits. *Proc Natl Acad Sci U S A* 99: 5878–5883.
33. Gottschalk KE (2005) A coiled-coil structure of the alphaIIb beta3 integrin transmembrane and cytoplasmic domains in its resting state. *Structure* 13: 703–712.
34. Metcalf DG, Kulp DW, Bennett JS, DeGrado WF (2009) Multiple approaches converge on the structure of the integrin alphaIIb/beta3 transmembrane heterodimer. *J Mol Biol* 392: 1087–1101.
35. Suk JE, Situ AJ, Ulmer TS (2012) Construction of covalent membrane protein complexes and high-throughput selection of membrane mimics. *J Am Chem Soc* 134: 9030–9033.
36. Hughes PE, Diaz-Gonzalez F, Leong L, Wu C, McDonald JA, et al. (1996) Breaking the integrin hinge. A defined structural constraint regulates integrin signaling. *J Biol Chem* 271: 6571–6574.
37. Ahrens IG, Moran N, Aylward K, Meade G, Moser M, et al. (2006) Evidence for a differential functional regulation of the two beta(3)-integrins alpha(V)beta(3) and alpha(IIb)beta(3). *Exp Cell Res* 312: 925–937.
38. Abair TD, Bulus N, Borza C, Sundaramoorthy M, Zent R, et al. (2008) Functional analysis of the cytoplasmic domain of the integrin {alpha}1 subunit in endothelial cells. *Blood* 112: 3242–3254.
39. Palmer AG, 3rd (2004) NMR characterization of the dynamics of biomacromolecules. *Chem Rev* 104: 3623–3640.
40. Boehr DD, Dyson HJ, Wright PE (2006) An NMR perspective on enzyme dynamics. *Chem Rev* 106: 3055–3079.
41. Maltsev AS, Grishaev A, Bax A (2012) Monomeric alpha-synuclein binds Congo Red micelles in a disordered manner. *Biochemistry* 51: 631–642.
42. Vossmeier D, Kaufmann C, Loster K, Lucka L, Horstkorte R, et al. (2000) The cytoplasmic domain of the alpha1 integrin subunit influences stress fiber formation via the conserved GFFKR motif. *Exp Cell Res* 256: 321–327.
43. Loster K, Vossmeier D, Hofmann W, Reutter W, Danker K (2001) alpha1 Integrin cytoplasmic domain is involved in focal adhesion formation via association with intracellular proteins. *Biochem J* 356: 233–240.
44. Vossmeier D, Hofmann W, Loster K, Reutter W, Danker K (2002) Phospholipase Cgamma binds alpha1beta1 integrin and modulates alpha1beta1 integrin-specific adhesion. *J Biol Chem* 277: 4636–4643.